TRANSLATIONS                    CLB-3  T-647     21 April 1971

LONG-PERIOD SATELLITE PERTURBATIONS

UNDER THE ACTION OF SOLAR RADIATION PRESSURE
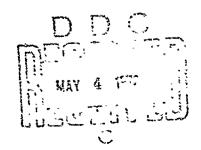
by

E. N. Polyakhova

translated by C. R. Haave from

Vestnik Leningradskogo Universiteta, Astronomiya

[Bulletin, Leningrad University, Astronomy]

No. 7, pp. 144-152 (1970)

## SUMMARY

The long-period perturbations of the orbital elements of
satellites caused by direct solar radiation pressure are considered
for satellites of high "area-to-mass" ratio. A series of orbits is
selected to illustrate the main perturbation effects. The graphs are
drawn up neglecting planet asphericity and the effects of shadowing.

Approved for public release; distribution unlimited.

DDC

MAY 4

17

## DOCUMENT CONTROL DATA - R & D

*(Security classification of title, body of abstract and indexing annotation must be entered when the overall report is classified)*

| 1 ORIGINATING ACTIVITY (Corporate author) | 2a. REPORT SECURITY CLASSIFICATION |
|---|---|
| The Johns Hopkins University, Applied Physics Lab. 8621 Georgia Avenue Silver Spring, Md. | Unclassified |
| | 2b. GROUP |

3 REPORT TITLE

Long-Period Satellite Perturbations Under the Action of Solar Radiation Pressure

4 DESCRIPTIVE NOTES (Type of report and inclusive dates)

5 AUTHOR(S) (First name, middle initial, last name)

E. N. Polyakhova

| 6 REPORT DATE | 7a. TOTAL NO. OF PAGES | 7b. NO. OF REFS |
|---|---|---|
| 21 April 1971 | | |

| 8a. CONTRACT OR GRANT NO. | 9a. ORIGINATOR'S REPORT NUMBER(S) |
|---|---|
| N00017-72-C-4401 | |
| b. PROJECT NO. | CLB-3 T-647 |
| c. | 9b. OTHER REPORT NO(S) (Any other numbers that may be assigned this report) |
| d. | |

10 DISTRIBUTION STATEMENT

This document has been approved for public release and sale; its distribution is unlimited.

| 11. SUPPLEMENTARY NOTES | 12. SPONSORING MILITARY ACTIVITY |
|---|---|
| | NAVPLANTREPO Naval Ordnance Systems Command |

13 ABSTRACT

The long-period perturbations of the orbital elements of satellites caused by direct solar radiation pressure are considered for satellites of high "area-to-mass" ratio. A series of orbits is selected to illustrate the main perturbation effects. The graphs are drawn up neglecting planet asphericity and the effects of shadowing.

DD FORM 1 NOV 65 1473

14.

KEY WORDS

Space science

Satellite perturbations

Solar radiation effects

Requester: E. L. Brickner

# LONG-PERIOD SATELLITE PERTURBATIONS
## UNDER THE ACTION OF SOLAR RADIATION PRESSURE[*)]

by

E. N. Polyakhova

Let us consider an artificial planetary satellite whose orbital position is fixed by the six Kepler elements $x_j$ (j = 1,2,...,6). The equation of the perturbed motion affected by light radiation pressure can be written as an equation in a small parameter

$$\frac{dx_k}{dt} = \sigma \varphi_k (x_j, \lambda_\odot, E) \quad \binom{k = 1, 2, \ldots, 6}{j = 1, 2, \ldots, 6}, \tag{1}$$

where $\sigma$, the ratio of the modulus of the perturbing acceleration to the gravitational parameter of the planet, serves as the small parameter. Equation (1) indicates that the right-hand terms contain the orbital elements, the sun's longitude $\lambda_\odot$ and the satellite's orbital eccentricity E.

Equation (1) may be integrated approximately using either Picard's method or the small-parameter method, since for an equation such as (1) the first and second approximations agree for both methods [1]. The transformation

$$\int_{t_*}^{t} \varphi_k (x_j^0, \lambda_\odot, E) \, dt = \int_{E_*}^{E} \frac{r}{na} \varphi_k (x_j^0, \lambda_\odot, E) \, dE, \tag{2}$$

where $x_j^0 = x_j$ (t = $t_0$) are the initial values of the elements, is useful in evaluating the integral. Explicit expressions for the right-hand terms of (1) are easily

obtained from the known differential equations of perturbed motion, the equations being in Newtonian form--i.e. containing components of the perturbing acceleration [2]. The perturbing acceleration will be defined by the formulas

$$\vec{F} = -F\vec{u^0}, \quad F = P_r \frac{A}{m},$$ (3)

where $P_r$ is the magnitude of the solar radiation pressure at the planet's orbit, $A/m$ is the "surface-to-mass" ratio of the satellite, $\bar{u}_0$ is a unit vector in the earth-sun direction. Formulas (3) correspond to a spherical satellite model, for which the force of the pressure is known not to depend on the reflectivity. It is convenient to define the components of the unit vector $\bar{u}^0$ in an orthogonal system of axes located at the pericenter of the satellite's orbit (radial, transverse and bi-normal directions). The derivations of these formulas may be found in reference [3]. We cite here the final expressions for the projections of the unit vector on these axes:

$$S = \sum_{i=1}^{6} A_i \cos \alpha_i, \quad T = -\sum_{i=1}^{6} A_i \sin \alpha_i, \quad W = \sum_{i=7}^{9} A_i \sin \alpha_i,$$

$$A_1 = \cos^2 \frac{i}{2} \sin^2 \frac{\varepsilon}{2}, \quad \alpha_1 = \omega + \Omega + \lambda_\odot,$$

$$A_2 = \sin^2 \frac{i}{2} \sin^2 \frac{\varepsilon}{2}, \quad \alpha_2 = \omega - \Omega - \lambda_\odot,$$

$$A_3 = \cos^2 \frac{i}{2} \cos^2 \frac{\varepsilon}{2}, \quad \alpha_3 = \omega + \Omega - \lambda_\odot,$$

$$A_4 = \sin^2 \frac{i}{2} \cos^2 \frac{\varepsilon}{2}, \quad \alpha_4 = \omega - \Omega + \lambda_\odot.$$ (4)

$$A_5 = -\frac{1}{2} \sin i \sin \varepsilon, \quad \alpha_5 = \omega \quad + \lambda_\odot,$$

$$A_6 = \frac{1}{2} \sin i \sin \varepsilon, \quad \alpha_6 = \omega \quad - \lambda_\odot,$$

$$A_7 = \sin i \sin^2 \frac{\varepsilon}{2}, \quad \alpha_7 = \quad \Omega + \lambda_\odot,$$

$$A_8 = \sin i \cos^2 \frac{\varepsilon}{2}, \quad \alpha_8 = \quad \Omega - \lambda_\odot,$$

$$A_9 = \cos i \sin \varepsilon, \quad \alpha_9 = \quad \lambda_\odot.$$

-2-

Formulas for the perturbations over a single revolution can be derived by integrating equation (1), taking (2) and (4) into account, with the condition that the orbital elements and the solar longitude can be considered to be constants to within acceptable accuracy over one revolution of the satellite:

$$\delta a = 2a^2\sigma\left[S\left(Q_1 + \frac{e}{1-e^2}Q_3\right) - T\left(Q_2 + \frac{e}{1-e^2}Q_4\right)\right],$$
$$\delta e = a^2\sigma(SQ_3 - TQ_4),$$
$$\delta i = -a^2\sigma W(Q_2\cos\omega - Q_1\sin\omega),$$
$$\delta\Omega = -\frac{a^2\sigma}{\sin i}W(Q_1\cos\omega + Q_2\sin\omega), \qquad (5)$$
$$\delta\omega = \frac{a^2\sigma}{e}(SQ_5 - TQ_6) - \cos i\,\delta\Omega,$$
$$\delta M_0 = 3\pi a^2\sigma eS - \sqrt{1-e^2}(\delta\omega + \cos i\,\delta\Omega) +$$
$$+ 2a^2\sigma\sqrt{1-e^2}(SQ_2 + TQ_1),$$

where the quantities $Q_i$ are defined by

$$Q_1 = \cos E - \frac{e}{4}\cos 2E,$$
$$Q_2 = \frac{1}{2\sqrt{1-e^2}}\left[3eE - 2(1+e^2)\sin E + \frac{e}{2}\sin 2E\right],$$
$$Q_3 = \frac{1}{4}(1-e^2)\cos 2E,$$
$$Q_4 = -\frac{1}{2}\sqrt{1-e^2}\left(3E - 4e\sin E + \frac{1}{2}\sin 2E\right), \qquad (6)$$
$$Q_5 = -\frac{1}{2}\sqrt{1-e^2}\left(3E - 2e\sin E - \frac{1}{2}\sin 2E\right),$$
$$Q_6 = -e\cos E + \frac{1}{4}\cos 2E.$$

Formulas (5) are convenient for calculating the perturbations over any number of orbital periods q, by recalculating the elements from revolution to revolution in accordance with the scheme

$$(x_k)_q = (x_k)_{q-1} + \delta x_k.$$

The quantities (6) must be calculated within the limits $E_2$ to $E_1$, which means that the integration is carried out over a complete period of change in E from 0 to $2\pi$,

from which we exclude the region of shadowing by the planet, when there is no acceleration perturbation. If the shadowing limits in the orbit are defined as points with the eccentric anomalies $E_1$ (entering) and $E_2$ (leaving), the integration must be carried out within the limits 0 to $E_1$, and from $E_2$ to $2\pi$ if the perigee ($E = 0$) lies in light ($E_2 - E_1 > 0$) and from $E_2$ to $E_1$ if the perigee lies in the shadow ($E_2 - E_1 < 0$).

Formulas (5) for the case of total illumination can be used for calculating the perturbations over one or a number of revolutions, or also over some portion of a revolution. Having obtained these, it is simple to follow the evolution of the orbit of satellites over long intervals of time by computing the elements from orbit to orbit. Since in these formulas the perturbing influence of the oblateness of the planet is not taken into account, the computed results will be close to the real picture of the evolution of very high orbits with uniform physical characteristics of the satellite and for lighter satellites during single orbits.

In this paper we investigate the long-period perturbations of the satellite orbital elements. We shall not consider short-period perturbations caused by shadowing effects. The sequence for comparing the evolution of the orbits is as follows: we first set up the model of a light spherical satellite ($A/m = 200$ $cm^2/g$) and consider the perturbations for orbits of different dimensions and orientations around the earth; second, we consider different satellites to study the influence of the parameter $A/m$; third, we examine two identical satellite orbits for Earth and Mars (with like parameters $A/m$) to compare the satellite perturbations for different planets.

We now turn to perturbations of earth satellites ($P_r = 0.46 \times 10^{-4}$ $g/cm \cdot sec^2$) and examine separately the perturbations of various periods. It follows from the form of formula (4) that the perturbation periods are determined by the rates of

change of the quantities $\lambda_\omega$, $\pi$, $i$, $\Omega$. Obviously, we must first of all consider the yearly periodicity related to solar motion; this is conveniently done by varying the elements $e$ and $\omega$, which are subjected to the largest relative changes due to radiation pressure of the elements. The elements $i$ and $\Omega$ are changed rather weakly over the course of a year (especially with small values of $e$), since $e$ appears linearly in the coefficient in the year term in $Q_2$. The semi-major axis $a$, in general, does not change with full illumination. The change in $M_0$ is determined basically by the change in $\pi$ and will not be considered individually.

Dependence on Semi-major Axes. Let us consider an orbit with the elements $e_0 = 0.1$, $i_0 = 5^0$, $\Omega_0 = \omega_0 = \lambda_0 = 0^0$. Figs. 1 and 2 show graphically the changes in $e$ and $\pi$ over a year for the following values of $a$: 24,000, 21,400, 13,500, 7,400 km, as computed using formula (5). The curves of $e(a)$ show the annual oscillation, with the curve changing from convex-upward to convex-downward (the results of the calculations for $a = 42,000$ km are in agreement with the data of references [4] and [5]). As the computations for other initial data showed, as $e_0$ increases the entire set of curves will have a tendency to fall lower. For each value of $e_0$ it is possible to select a value of $a$ for which a minimum change in $e$ is observed (for example, $0.1 \leq e \leq 0.2$, 13,000 km $\leq a \leq 42,000$ km). The shape of the eccentricity curves repeats from year to year. The perigee (Fig.2) moves in an annual circle with variable velocity, making a full revolution per year (the straight line denotes the change in longitude of the sun). With large values of $e_0$ or small values of $A/m$ the perturbations in $\omega$, as follows from (5), will be small and will show up as oscillatory (loop-shaped) motion around the initial position.
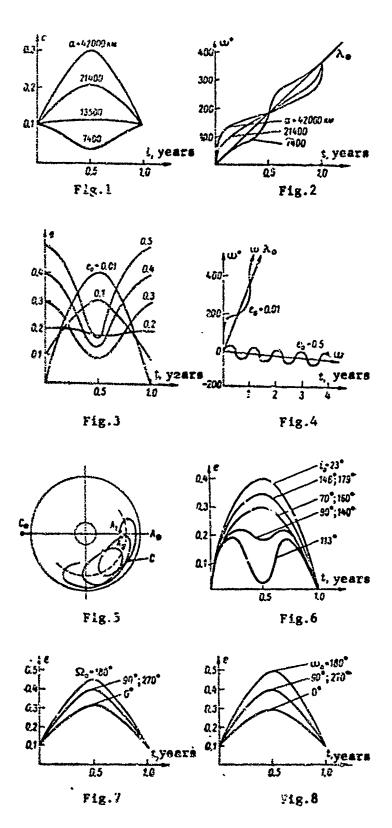
Dependence on Eccentricity. Let us select an orbit close to synchronous: $a = 42,000$ km, $i_0 = 5^0$, $\pi_0 = \Omega_0 = \lambda_0 = 0^0$. Figs. 3 and 4 show graphs of $e$ and $\omega$ for a series of $e_0$: 0.01, 0.1, 0.2, 0.3, 0.4 and 0.5. Again we see three types of curve for $e(e_0)$: for $e_0 \leq 0.32$ the perigee moves in a forward motion; for $e > 0.32$ the

motion reverses. For $e_0 = 0.5$ the perigee moves with a counter loop-shaped motion, making a complete revolution in 22 years. Fig. 5 illustrates such a perigee path over a period of 4 years: points $A_1$ and $A_2$ are separated by year intervals, $A_\odot$ is the sun · position at these times. As will be shown below, the perigee motion for the next 22 years will be exactly the opposite since the total period of change is 44 years (for a synchronous satellite).

Influence of Inclination. For orbits with $a = 42,000$ km, $e_0 = 0.01$, $i_0 = \Omega_0 = \omega_0 = 0°$ we examine a series of inclinations $i_0 = 1°$, $23°$, $46°$, $70°$, $90°$, $11°$, $'40°$, $160°$ and $179°$. All curves of $e(i_0)$ (Fig.6) are distributed in a region ...... by the two curves $e(i_1 \approx \epsilon \approx 23°)$ and $e(i_2 \approx 90° + \epsilon \approx 113°)$, where the curves for values of $i_0$ symmetrical with respect to $i_1$ or $i_2$ must coincide. This regularity is observed for any choice of initial elements, although the shape of the $e(i_0)$ curves will in this case be altered.

Effect of Nodal Longitude and Argument of Perigee. Let us select two identical orbits: $a = 42,000$ km, $e_0 = 0.1$, $i_0 = 23.5°$, $\lambda_\odot^0 = 0°$. The effects of the annual variation in $i$ and $\Omega$ is completely excluded from the perturbations of $e$ and $\omega$ for such an orbit, since for $\Omega_0 = 0°$, $\delta i = \delta \Omega = 0°$ (ecliptic orbit), and these perturbations are small for $\Omega_0 \neq 0°$. We shall choose the values $\omega_0 = 0°$, $\Omega_0 = 0°$, $90°$, $180°$, $270°$ (Fig. 7) and $\Omega_0 = 0°$, $\omega_0 = 0°$, $90°$, $180°$, $270°$ (Fig.8). It is apparent that the evolution of the elements is not affected by the actual values of $\Omega_0$ or $\omega_0$, but by the mutual initial disposition of node and perigee. The inequality of amplitudes in Figs. 7 and 8 indicates that $\Omega$ and $\omega$ enter in quite different ways into the equation.

Influence of Solar Longitude. Let us consider a synchronous orbit: $a = 42,000$ km, $e_0 = 0.1$, $i_0 = 23.5°$ (ecliptic), $\omega_0 = \Omega_0 = 0°$. The curves of $e$ and $\omega$ $(\lambda_\odot^0 = 0, 180°)$ coincide, and the curves of $e$ and $\omega$ $(\lambda_\odot^0 = 90°, 270°)$ are symmetrically disposed relative to the straight line $\tau = P/2$ (Figs. 9 and 10). In the

$c$

$a=42000\,\text{km}$

$0.3$

$21400$

$0.2$

$13500$

$0.1$

$7400$

$t$, years

$0.5$    $1.0$

**Fig.1**

$\omega^\circ$

$400$

$\lambda_\oplus$

$300$

$200$

$a=42000\,\text{km}$

$21400$

$100$

$7400$

$t$, years

$0.5$    $1.0$

**Fig.2**

$e$

$0.5$

$0.4$

$e_0=0.01$

$0.4$

$0.3$

$0.1$

$0.3$

$0.2$

$0.2$

$0.1$

$t$, years

$0.5$    $1.0$

**Fig.3**

$\omega^\circ$   $\omega$   $\lambda_\oplus$

$400$

$200$

$e_0=0.01$

$e_0=0.5$

$0$    $\omega$

$-200$

$t$, years

$1$   $2$   $3$   $4$

**Fig.4**

$C_\oplus$   $A_1$   $A_\oplus$   $C$

**Fig.5**

$e$

$0.4$

$i_0=23^\circ$

$146^\circ; 179^\circ$

$0.3$

$70^\circ; 160^\circ$

$90^\circ; 140^\circ$

$0.2$

$0.1$

$113^\circ$

$t$, years

$0.5$    $1.0$

**Fig.6**

$e$

$0.5$

$\Omega_0=180^\circ$

$0.4$

$90^\circ; 270^\circ$

$0^\circ$

$0.3$

$0.2$

$0.1$

$t$, years

$0.5$    $1.0$

**Fig.7**

$e$

$0.5$

$\omega_0=180^\circ$

$90^\circ; 270^\circ$

$0.4$

$0^\circ$

$0.3$

$0.2$

$0.1$

$t$, years

$0.5$    $1.0$

**Fig.8**
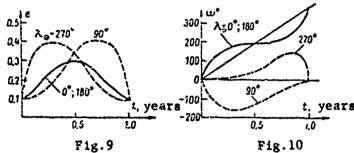
general case of arbitrary eccentricity the curves for $\lambda_{\odot}^0 = 0^0$ and $180^0$ are symmetrically disposed relative to the straight line $e_0$ = const. On the whole the asymmetry is determined by the asymmetry in the positions of perigee and the sun.

Let us now examine the longer-period perturbations. Here we shall consider the behavior of the elements i and $\Omega$ when the amplitudes of the corresponding variations of e and $\omega$ are small compared to their annual amplitude (the ordinates of the maxima of e exhibit only a weak long-period trend). The annual changes in e, $\omega$, and $\lambda_{\odot}$ exert an influence on i and $\Omega$ in the form of weak annual variations superposed on the main trend. These variations will not be shown on the following graphs.
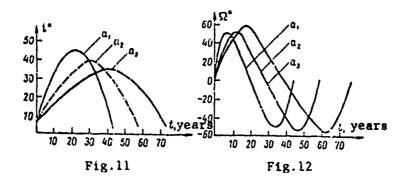
Fig.9              Fig.10

The variation of i and $\Omega$ without taking shadowing into account is defined by the formulas

$$\frac{di}{dt} = -\frac{3}{2}\frac{na^2 c_3}{\sqrt{1-e^2}} W \cos \omega, \quad \frac{d\Omega}{dt} = -\frac{3}{2}\frac{na^2 c_3}{\sin i \sqrt{1-e^2}} W \sin \omega, \tag{7}$$

where

$$W = \sin i \sin^2 \frac{\varepsilon}{2} \sin (\Omega + \lambda_{\odot}) + \sin i \cos^2 \frac{\varepsilon}{2} \sin (\Omega - \lambda_{\odot}) + \\ + \cos i \sin \varepsilon \sin \lambda_{\odot}.$$
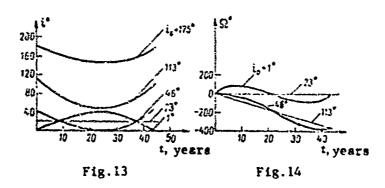
It is clear from (7) that we have, as a function of the arguments of the trigonometric terms, either the annual variations due to changes in $\lambda_{\odot}$, or the variations arising from the superposition of variations with periods $2\pi : \frac{di}{dt}$ and $2\pi : \frac{d\Omega}{dt}$. Since these derivatives are small the oscillation periods can be quite long.

-8-

Fig.11          Fig.12

Influence of Semi-axis. We choose an elliptical orbit, near equatorial ($e_0 = 0.1$, $i_0 = 5^0$, $\omega_0 = \Omega_c = \lambda_\odot^0 = 0^0$) and vary the semiaxis: $a_1 = 42,000$ km, $a_2 = 23,000$ km, $a_3 = 13,500$ km. From the formulas it follows that the amplitudes should be related as $\sqrt{a}$ and the periods as $1/\sqrt{a}$.
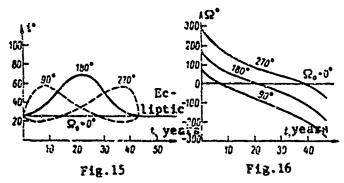
Graphs of the variations in $i$ and $\Omega$ are shown in Figs. 11 and 12. The amplitudes are related as 2.5:2:1.5, the periods as 4:5.2:6.7. The minimum period represents a stationary orbit -- 44 years. The variations in the other elements will be considered just for this period.

The Influence of Elements having an Annual Period of Variation. Among these quantities are e, $\omega$ and $\lambda_\odot$. By virtue of the fact that $\lambda_\odot$ has no annual periodicity and it is negligibly small for e and $\omega$, these elements exert no appreciable effect on the course of $i$ and $\Omega$. Calculations for the stable orbit yield almost identical curves and therefore we shall not reproduce them here. This is observed even for large values of e, when the annual movement in $\omega$ is appreciable.
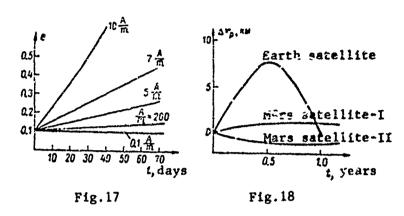


Fig.13          Fig.14

-9-

Influence of Inclination. The elements i and $\Omega$ react strongly on the variation in $i_0$ and their plots differ for different values of $i_0$. Let us again consider the orbit: a = 42,000 km, $e_0$ = 0.01, $\omega_0$ = $\Omega_0$ = $\lambda_\odot^0$ = $0^\circ$. All equatorial and near- equatorial orbits show an increase in i proportional to $1/\sin i$ (Fig. 13) until, finally, the curve of i ($i_0 \approx \varepsilon$) reduces to a straight line (W = 0, $\delta i$ = $\delta \Omega$ = 0). For all $i_0 > \varepsilon$, i begins to decrease, with the maximum amplitude of the decrease corresponding to $i_0 \approx 90^\circ + \varepsilon \approx 113^\circ$, since $W(i_0 \approx 90^\circ + \varepsilon)$ = $\cos \varepsilon \sin \lambda_\odot$ ($\cos \varepsilon + \sin \varepsilon$) has a maximum. Then the amplitudes decrease and the curves $i(i_0 = 170^\circ)$ and $i(i_0 = 1^\circ)$ are symmetrical around the line $i_0 = 90^\circ$. The curves of $\Omega(i_0)$ (Fig. 14) show a long-period counter motion of the node for $i_0 > \varepsilon$ and a loop-shaped motion for $i_0 < \varepsilon$. The node of the elliptical orbit is stationary. The distribution of curves by amplitude is preserved for any value of $\Omega_0$ but the symmetry is lost.

Influence of Node Longitude. Let us select a stationary, ecliptic orbit. In this case we observe complete symmetry of the curves i ($\Omega_0$ = $0^\circ$, $180^\circ$) for both half-periods, where $\delta i(\Omega = 0)$ = 0 since W = 0. The curves $i(\Omega_0 = 90^\circ, 270^\circ)$ pass through each other on rotation around the axis t = P/2 (Fig. 15). In the case $\Omega_0$ = $0^\circ$ we again have $\delta \Omega$ = 0 (Fig. 16), and for other values of $\Omega_0$ the node motion is in the opposite direction with variable velocities. The entire set of curves $i(\Omega_0)$ for equatorial orbits should be stretched out upward, and the rate of change of $\Omega(\Omega_0)$ should vary more strongly. In the case of a polar orbit the curves $i(\Omega_0 = 0^\circ, 180^\circ)$ should be rigorously symmetrical with respect to $i_0$ = const, and the rate of movement of the node should be almost constant.



Fig.15          Fig.16

Let us now examine the influence of the parameter A/m on the development
of the orbital elements. Until now we have varied the orbital elements of earth
satellites with the same value of $A/m = 200 \text{ cm}^2/g$, and have considered this to be
a fixed quantity. Let us now set up a single orbit ($a = 42,000$ km, $e_0 = 0.01$,
$i_0 = 5^0$, $\omega_0 = \Omega_0 = \lambda_\odot^0 = 0^0$) and select certain values of A/m (A/m = 200:0.1 A/m,
5 A/m, 7 A/m, 10 A/m). Fig. 17 shows curves of the change in eccentricity over a



Fig.17                    Fig.18

2-month interval. From these curves we can form a conclusion regarding the magni-
tude of the changes in the remaining orbital elements. In the calculations we used,
as before, the spherical satellite model with constant A/m. For this satellite
the question of orientation relative to the solar radiation during the course of
the year does not arise. In addition, the acceleration of a spherical satellite
does not depend on its surface reflectivity (with geometrical reflection properties).
In the general case the object with constant A/m may be a satellite of arbitrary
shape that preserves its orientation relative to the sun. If the orientation of
the satellite is arbitrary, the law of the change in illuminated surface should be
given functionally, as was done, for example, in reference [5] for synchronous sate-
llites. Here we must keep in mind that the acceleration F of any satellite will lie
in the range

$$F_s < F \leqslant F_p$$

where $F_s$ is the acceleration of a sphere and $F_p$ is the acceleration of a flat plate

-11-

whose illuminated surface is equal to the central cross section of the sphere and of the arbitrary satellite. In this case we compute the acceleration from the formulas

$$F_s = P_r \frac{A}{m}, \quad F_p = \sqrt{F_n^2 + F_\tau^2},$$
$$F_n = (1 + \epsilon) P_r \cos^2 \vartheta \frac{A}{m}, \quad F_\tau = (1 - \epsilon) P_r \sin \vartheta \cos \vartheta \frac{A}{m},$$

where $\epsilon$ is the coefficient of reflection, $\vartheta$ is the angle of incidence, $F_n$ and $F_\tau$ are the normal and tangential components of the pressure.

In order to compare the perturbations of individual satellites for two planets, let us consider satellites orbiting Earth and Mars. For comparison purposes we select a heavy satellite (A/m = 0.1 cm$^2$/g) in an orbit with the elements a = 42,000 km, $e_0$ = 0.01, $i_0$ = 5°, $\omega_0$ = $\Omega_0$ = $\lambda_\odot^0$ = 0°. For the earth this is close to an actual synchronous satellite. Fig. 18 shows curves of the change in the perigee radius-vector in the course of a year. The maximum amplitude for the earth amounts to about 7 km. The corresponding amplitudes in $\omega$ are ±1° per year; the perigee executes small oscillations around the stable position, so that a longitude shift of the satellite is not expected. The middle curve of Fig. 18 shows $\Delta r_p$ for a satellite of Mars; the annual amplitude does not exceed 0.5 km. This difference is explained by the fact that the value of $P_r$ in the Mars orbit is about half that in the Earth orbit, which is close to the synchronous orbit (a $\approx$ 20,000 km). We present a table of some values taken from the calculations made for the curves of Fig. 18.

| | Earth | Mars |
|---|---|---|
| $P_r, \dfrac{g}{cm \cdot sec^2} \left[\dfrac{dynes}{cm^2}\right]$ | $0.45 \cdot 10^{-4}$ | $0.20 \cdot 10^{-4}$ |
| $F$, cm/sec$^2$ | $0.45 \cdot 10^{-5}$ | $0.20 \cdot 10^{-5}$ |
| $R$, км | 6371 | 3407 |
| $fM$, км$^3$/ sec$^2$ | 398 600 | 42 900 |
| $\epsilon^0$ | 23°5 | 25°0 |
| $\lambda_\odot$, deg/day | 0.98565 | 0.52500 |

## References

1. G.N. Duboshin. Nebesna;a mekhanika (Celestial Mechanics); Moscow, "Nauka" (1963).

2. M.F. Subbotin. Vvedenie v teoreticheskuyu astronomiyu (Introduction to theoretical astronomy); Moscow, "Nauka" (1968).

3. E.N. Polyakhova. Radiation pressure and the motion of earth satellites, Bylleten' ITA; 9, No. 1, Issue 104 (1963).

4. E. Lewin. Solar radiation pressure perturbations of earth satellite orbits, AIAA J.; 6, No. 1 (1968).

5. A.G. Lubowe. Orbital behaviour of large synchronous satellites, Astronaut. Acta; 13, No. 1 (1967).

6. Y. Kozai. Effects of solar radiation pressure on the motion of an artificial satellite. Smith. Astrophys. Obs.; Special Report 56 (1961).

7. I.I. Shapiro. The prediction of satellite orbits, Symposium on dynamics of satellites; Paris (1962).